

Search for Massive Bosons Decaying to $W\gamma$ and $Z\gamma$ Using the ATLAS Detector

Wei Tang
Department of Physics
Duke University

Contents

1	Introduction	2
2	Leptonic Decay	2
2.1	Event Selections	3
2.2	Signal Simulation	3
2.3	Background Simulation	4
3	Hadronic Decay	5
3.1	Event Selections	6
3.2	Selection Efficiencies	7
3.3	Decay Polarizations	8
4	Conclusion	12

1 Introduction

The Standard Model is by far the most encompassing physics theory. With the recent discovery of the Higgs Boson, the Standard Model has performed extremely well against experimental data. However, the theory is intrinsically not complete, it does not address physical phenomenon such as gravity and dark matter. Many proposals for physics beyond the Standard Model predict new massive bosons from additional gauge fields or extended Higgs sectors.

At CERN, we analyze proton-proton collision experimental data to search for evidence of new particles. This paper examines possible decay channels of an unknown massive boson X decaying into V plus a gamma, where V can be either a W or a Z boson. The production mechanism can be either gluon-gluon fusion or $q - \bar{q}$ annihilation. Figure 1 illustrates the possible production and decay channels.

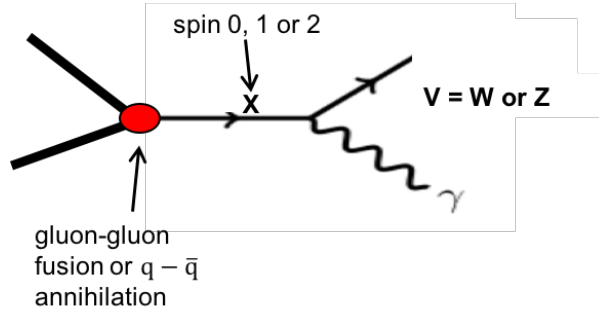


Figure 1: $X \rightarrow V\gamma$

The data being analyzed in this paper is collected by the ATLAS detector at the CERN Large Hadron Collider. The data comes from proton-proton collisions with a center of mass energy of 13TeV, and has a total integrated luminosity of 36.1 fb^{-1} . The data is collected using a trigger based upon a photon with transverse energy greater than 140 GeV.

This paper describes preliminary results from a generic search for new massive X bosons. The ultimate goal of our search is to explore the X mass range from 250 GeV to highest energy attained in 13TeV p-p collision.

2 Leptonic Decay

The boson decay products from the unknown massive boson X can further undergo either leptonic or hadronic decay. In the leptonic decay, the Z boson further decays into a pair of either electron and positron or $\mu^+ \mu^-$.

2.1 Event Selections

The leptonic decay events were selected using single electron and muon triggers with a nominal transverse momentum larger than 26 GeV, supplemented by di-lepton triggers with lower thresholds.

The Z bosons which decay to a pair of leptons are selected using well measured, isolated electron and muon pairs with invariant mass within ± 15 GeV of the invariant mass of Z bosons.

The photons are required to be isolated with pseudo rapidity $|\eta| < 1.37$ or $1.52 < |\eta| < 2.37$ and transverse momentum $P_T > 10$ GeV. These requirements ensure that we are using the detector region with highest granularity.

The final $Z\gamma$ event selection requires the photon to have transverse momentum greater than 30% of the combined $Z\gamma$ invariant mass.

2.2 Signal Simulation

In the signal simulation, unknown massive boson X decays with a narrow width to a Z boson and γ . The narrow width chosen is 4 MeV. Figure 2 on page 3 shows the $Z\gamma$ combined invariant mass distribution with all selection cuts applied.

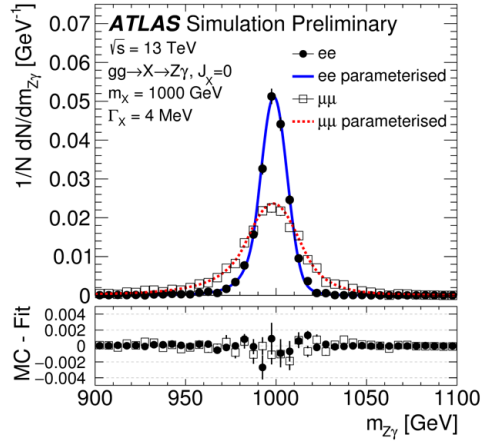
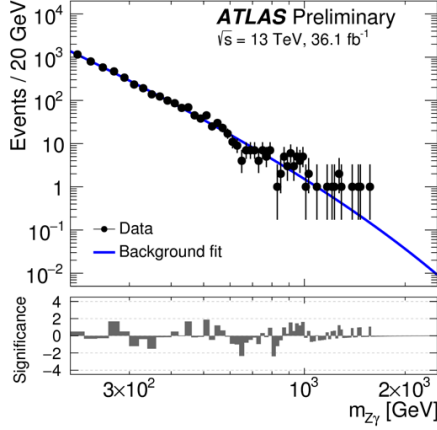
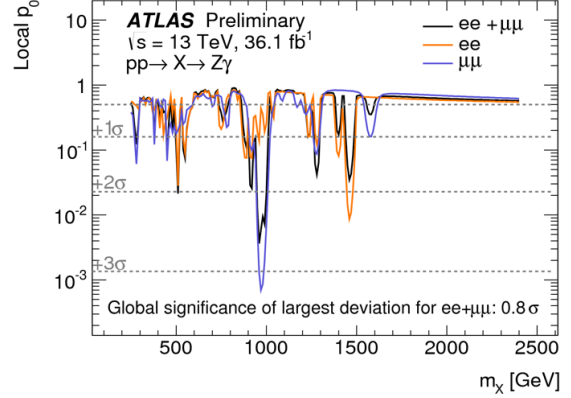


Figure 2: $Z\gamma$ Invariant Mass Simulation

Figure 3 on page 4 shows the total signal efficiency as a function of M_X . The signal efficiency of all the selection cuts combined range from 30-50% for increasing M_X .



(a) $M_{Z\gamma}$ Background Only Fit



(b) p-value of the $M_{Z\gamma}$ Distribution

Figure 4: Significance of $M_{Z\gamma}$ Observations

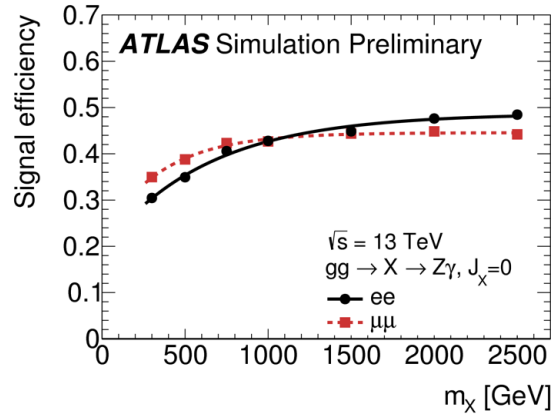


Figure 3: Simulation Signal Efficiency

Event samples are generated using POWHEG-BOX interfaced with Pythia, with M_X ranges from 200 GeV to 2.4 TeV.

2.3 Background Simulation

There are two sources of background. The dominant background is the Standard Model production of a Z boson plus a photon, with smaller contributions from Z + jets with the hadronic jet misidentified as a photon.

The $Z\gamma$ invariant mass data points are plotted with the background-only fit, as shown in Figure 4a on page 4. The solid blue line is the background prediction and black

dots are the actual data. The background $Z\gamma$ mass spectrum is smoothly falling and can be parameterized with $f(x) \approx (1 - x^{1/3})^{p_1} x^{p_2}$ with $x = M_{Z\gamma}/\sqrt{s}$. Figure 4b on page 4 shows the local p-value of the $M_{Z\gamma}$ data with respect to the background-only hypothesis. By comparing the data and the background, the largest local deviation is around $M_x = 268\text{GeV}$ where the local significance is 2.2σ .

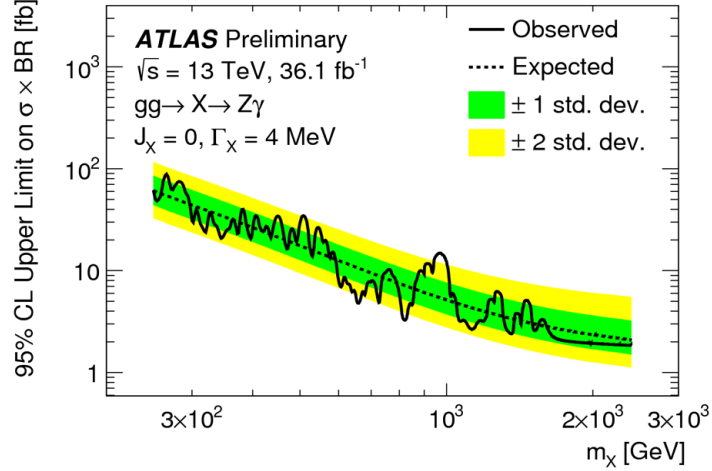


Figure 5: Confidence Level Limit

Upper limits on $\sigma(pp \rightarrow X) \times BR(X \rightarrow Z\gamma)$ are set using a profile likelihood method. Figure 5 on page 5 shows the observed (solid lines) and median expected (dashed lines) 95% confidence level limits on the product of the production cross section times the branching ratio for the decay to a Z boson and a photon of a narrow scalar boson X, $\sigma(pp \rightarrow X) \times BR(X \rightarrow Z\gamma)$. The green and yellow band indicate 1 and 2 standard deviation intervals. A modified frequentist (CLs) method is used to set upper limits on the product, by identifying the value of $\sigma \times BR$ for which $CL_s = 0.05$. The observed $\sigma \times BR$ limits vary from 88 fb at $M_X = 250$ GeV to 2.8 fb at $M_X = 2.40$ TeV. There is not a significant deviation from the observed $\sigma \times BR$ limits.

3 Hadronic Decay

The hadronic decays of the W/Z bosons have much higher branching ratio than the leptonic decays. The search sensitivity for $X \rightarrow W/Z + \gamma$ can be improved by capturing a higher fraction of the W/Z bosons from their hadronic decays. The branching ratio of $W/Z \rightarrow q\bar{q}$ is around 70%. Figure 6 on page 6 shows the production and decay channels.

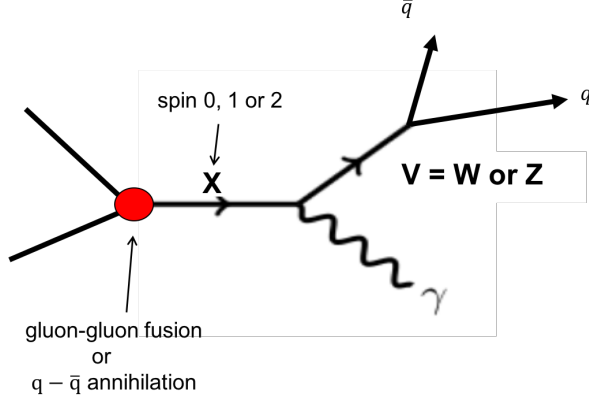


Figure 6: Hadronic Decay Channel

3.1 Event Selections

This search uses a selection of events based upon a photon trigger with transverse momentum $P_T > 140 \text{ GeV}$, followed by identification of highly boosted $W/Z(q\bar{q})$ bosons using fat jets with cone size $R = 1.0$. A jet substructure variable $D_2^{(\beta=1)}$ is used to identify fat jets with 2-jet substructure, to select hadronically decaying W/Z bosons while suppressing jets from single quarks or gluons. Figure 7 on page 6 shows the $q\bar{q}$ decays from a single W/Z boson. Due to the high momentum of the W/Z boson, the $q\bar{q}$ decay products are very close together and their subsequent shower merge.

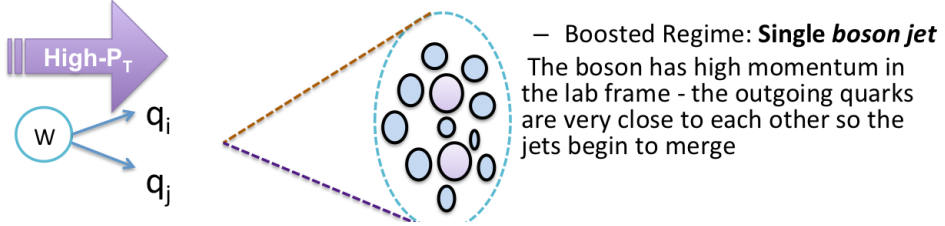


Figure 7: Identification of W/Z Boosted Jets

The spin 0 gluon-gluon fusion production with $Z\gamma$ decay signals are generated using the POWHEG-BOX generator. Both spin 1 $X \rightarrow W(q\bar{q}) + \gamma$ and spin 2 $X \rightarrow Z(q\bar{q}) + \gamma$ signals are generated using the MadGraph generator. The selection efficiency of the fat-jet identification of the W and Z bosons depends on the $\Delta R(q\bar{q})$ decay distribution, and is therefore sensitive to the polarization of the W/Z bosons. This paper studies the signal efficiency as a function of the X boson

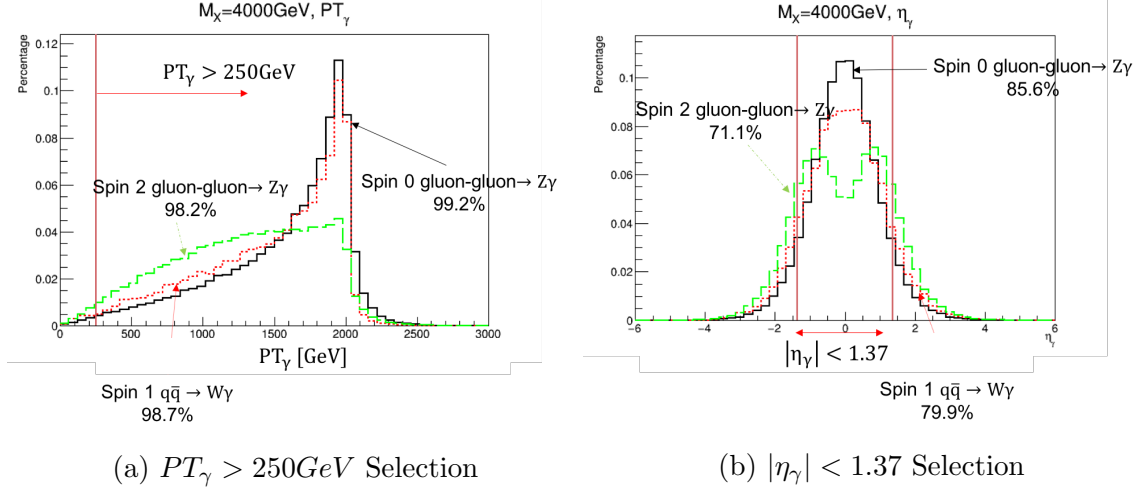


Figure 8: γ Kinematics Selection Cuts

mass using preliminary kinematic selection criteria. The kinematic selection criteria are:

1. $|\eta_{(q\bar{q})}| < 2$
2. $PT_{(q\bar{q})} > 200\text{GeV}$
3. $PT_\gamma > 250\text{GeV}$
4. $|\eta_\gamma| < 1.37$

3.2 Selection Efficiencies

Figures 8 and 13 show the selection efficiencies for the preliminary kinematic cuts applied separately on the signal events. The examples shown here are for $M_X=4\text{TeV}$. The same selection cuts are applied to signal events of all M_X slices. Figure 10 shows the total signal efficiencies from applying the combined kinematic selection cuts as a function of M_X for the three different hadronic channels. The signal efficiencies increase abruptly from low M_X to high masses.

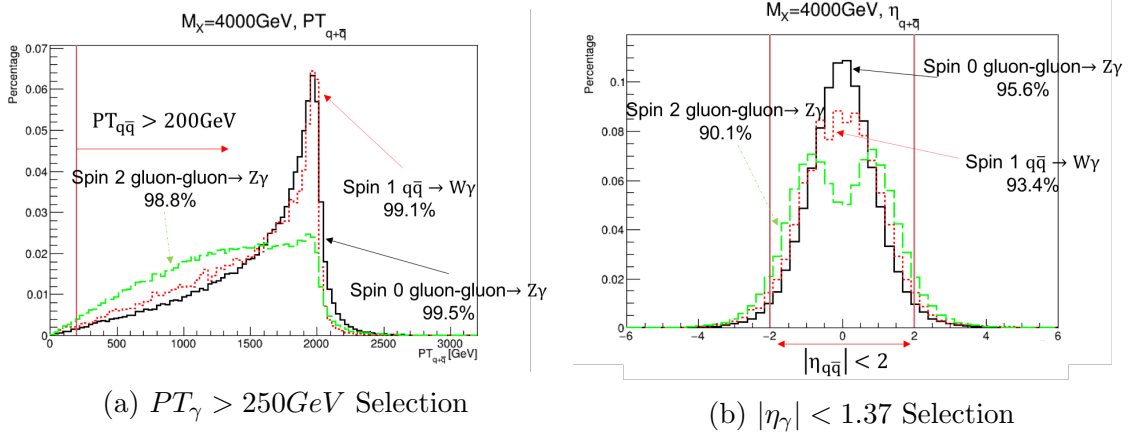


Figure 9: $q\bar{q}$ Kinematics Selection Cuts

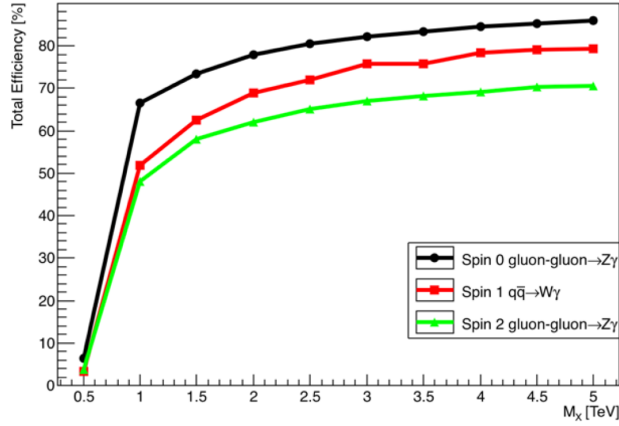


Figure 10: Signal Efficiency from Combined Kinematic Selection Cuts on All Three Production Channels

3.3 Decay Polarizations

The identification of W/Z boosted jet is affected by $\Delta R(q\bar{q})$ distributions and hence the polarizations of the boson decay products. In order to quantify such decay, this paper defines a helicity frame and analyzes the $q\bar{q}$ decay angular polarizations in the frame.

Figure 11 illustrates the definition of the helicity frame. The helicity frame is the W/Z boson rest frame with its Z axis defined to be along the same direction as the W/Z boson decay from the rest frame of massive boson X. We can reach the helicity

frame by performing two consecutive sets of rotation and boost from the proton-proton rest frame. In the helicity frame, the $q\bar{q}$ decay products are back to back due to conservation of momentum. This paper studies the $\cos\theta$ distribution to quantify the polarizations.

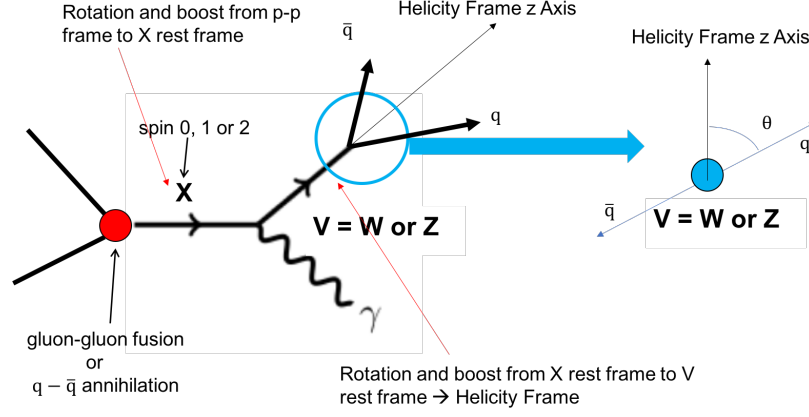


Figure 11: Helicity Frame Definition

Theoretically, the $\cos\theta$ distributions are different for the different W/Z production channels. Figure 12 shows the expected functional forms of the decay angular distributions from Standard Model electroweak decay of the W boson.

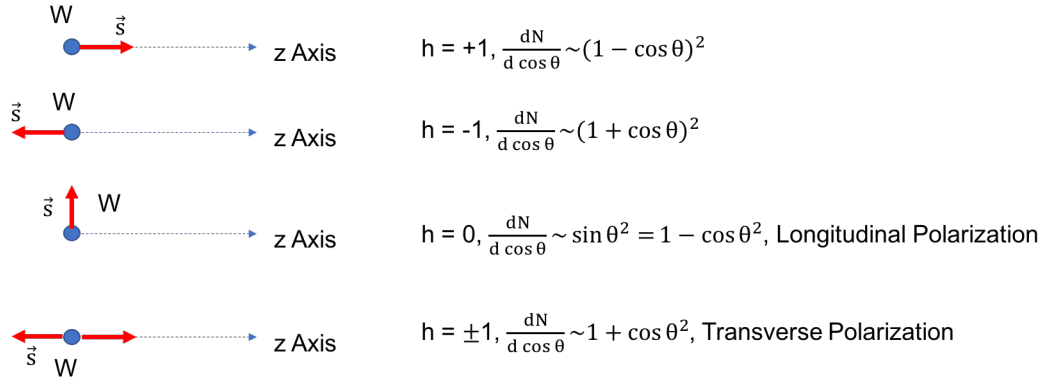
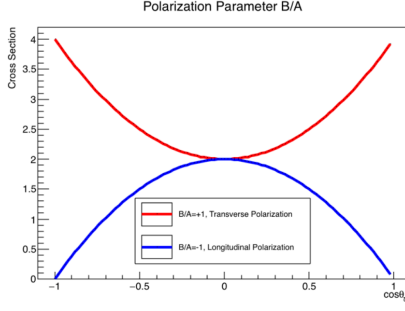
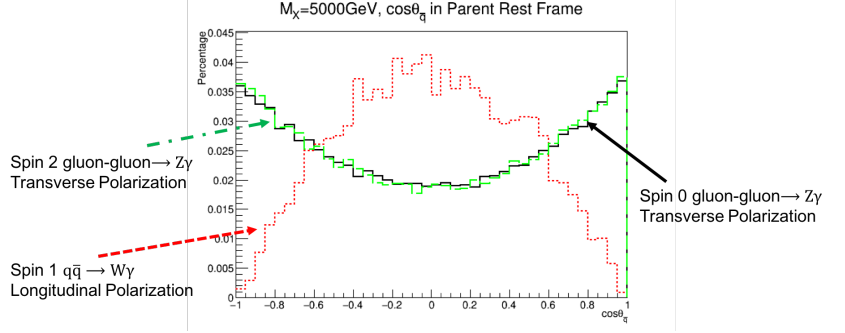


Figure 12: Functional forms of decay polarizations for different W/Z production channels

The $\cos\theta_{\bar{q}}$ distributions are fitted to the functional forms of $A + B\cos^2\theta = A(1 + \frac{B}{A}\cos^2\theta)$. The fitting parameter $\frac{B}{A}$ is hence used to quantify the polariza-



(a) $\cos \theta$ Distributions for purely longitudinal (blue) and purely transverse (red) polarizations



(b) $\cos \theta$ Distributions for three channels at $M_X=5\text{TeV}$

Figure 13: Theoretical $\cos \theta$ distributions and an example distribution

tion. $\frac{B}{A} = 1$ indicates a purely transverse polarization whereas $\frac{B}{A} = -1$ indicates a purely longitudinal polarization. Figure 13a illustrates the distributions for purely longitudinal and purely transverse polarizations. Figure 13b shows an example of $\cos \theta$ distributions at $M_X=5\text{TeV}$. It clearly demonstrates that the spin 0 and spin 2 productions are much more transversely polarized, while the spin 1 production is much more longitudinally polarized. The same fitting process is repeated for all M_X slices and the $\frac{B}{A}$ parameters as a function of M_X are plotted in Figure 14. Spin 0 and spin 2 productions are almost purely transversely polarized while the spin 1 production is almost purely longitudinally polarized.

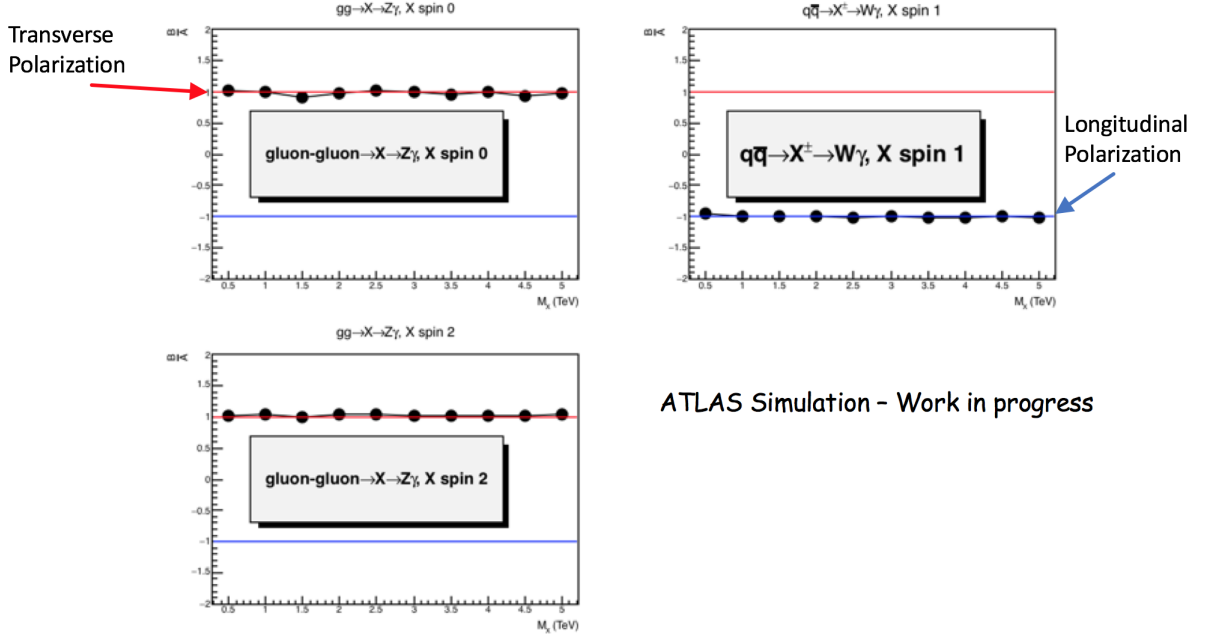


Figure 14: $\frac{B}{A}$ polarization parameter for all M_X

We use fat jet selection to identify W/Z boosted jet. This is using a cone radius of $\Delta R_{q\bar{q}} < 1$, which is defined to be

$$\Delta R_{q\bar{q}} = \sqrt{\Delta \eta_{q\bar{q}}^2 + \Delta \varphi_{q\bar{q}}^2} \quad (1)$$

Figure 15 shows the $\Delta R_{q\bar{q}}$ distributions for two M_X at 1TeV and 4TeV. We obtain good containment on the parton level. However, real data has extra inefficiencies due to presence of jets.

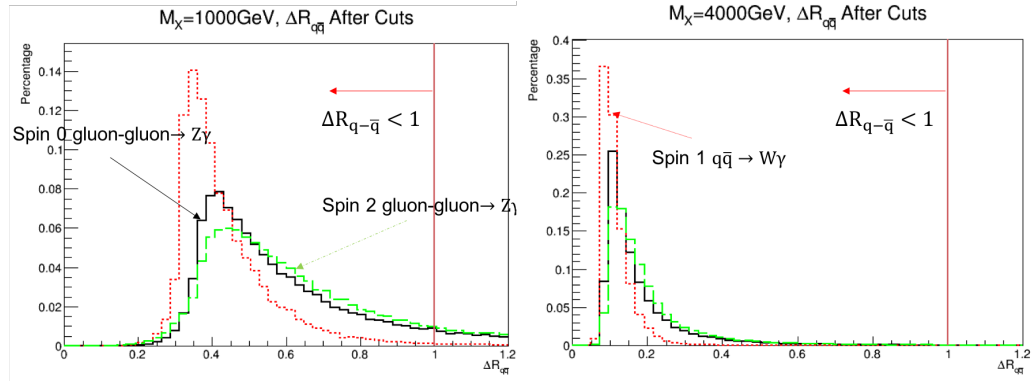


Figure 15: $\Delta R_{q\bar{q}}$ distributions for $M_X = 1 \text{ TeV}, 4 \text{ TeV}$

4 Conclusion

The ATLAS collaboration is carrying out a broad search for high mass bosons decaying to $Z\gamma$ and $W\gamma$ final states. Preliminary results using $36.1 fb^{-1}$ of data have been analyzed and place cross section limits on spin 0 production of $X \rightarrow Z\gamma$ with Z decays to e^+, e^- and μ^+, μ^- pairs. The limits for $\sigma_X \times BR(X \rightarrow Z\gamma)$ range between 88 fb for $M_X = 250$ GeV and 2.8 fb for $M_X = 2.4$ TeV.

The search sensitivity will be improved by including highly boosted W/Z bosons with hadronic decays. Preliminary studies have been done to determine selection cuts for spin 0 and spin 2 $X \rightarrow Z\gamma$ and spin 1 $X \rightarrow W\gamma$ decays. These show the potential for extending the search sensitivity for $X \rightarrow V\gamma$ decays for higher X masses.

References

- [1] HIGG-2016-14
- [2] A. J. Larkoski, I. Mould and D. Neill, Power Counting to Better Jet Observables, JHEP 1412 (2014) 009, arXiv: 1409.6298 [hep-ph].
- [3] A. J. Larkoski, G. P. Salam and J. Thaler, Energy Correlation Functions for Jet Substructure, JHEP 1306 (2013) 108, arXiv: 1305.0007 [hep-ph].